DOI: 10.1002/ejic.201100464

Facile Routes to Th^{IV}, U^{IV}, and Np^{IV} Phosphites and Phosphates

Eric M. Villa,[a] Shuao Wang,[a] Evgeny V. Alekseev,*[a,b,c] Wulf Depmeier,[b] and Thomas E. Albrecht-Schmitt*[a]

Keywords: Radiochemistry / Actinides / Hydrothermal synthesis / Neptunium / Uranium / Thorium

Three actinide(IV) phosphites and a Np^{IV} phosphate, $An^{IV}(HPO_3)_2(H_2O)_2$ (An = Th, U, Np) and $Cs[Np(H_{1.5}PO_4)(PO_4)]_2$, respectively, were synthesized using mild hydrothermal conditions. The first three phases are isotypic and were obtained using similar reaction conditions. $Cs[Np(H_{1.5}PO_4)(PO_4)]_2$ was synthesized using an analogous method to that of $Np(HPO_3)_2(H_2O)_2$. However, this fourth phase is quite different in comparison to the other phases in both composition and structure. The structure of $Cs[Np(H_{1.5}PO_4)(PO_4)]_2$ is constructed from double layers of neptunium(IV) phosphate with caesium cations in the interlayer region. In contrast, $An(HPO_3)_2(H_2O)_2$ (An = Th, U, Np) form dense 3D networks. The actinide contraction is detected in variety of metrics obtained from single-crystal X-ray diffraction data. Changes in the oxidation state of the neptunium starting materials yield different products.

Introduction

The limited solubility of actinide phosphates, such as uranyl phosphates, plays an important role in our understanding of how actinides migrate through the environment, be it from a natural deposit or from a geological repository for nuclear waste. Specifically, the fate of ^{237}Np is of concern in these repositories owing to its long half life of 2.14×10^6 years, and the fact that its amount actually increases in the short term owing to the α decay of ^{241}Am, which is also present in used nuclear fuel. ^{237}Np is responsible for most of the long term radioactivity from a repository if actinides are not removed from the fuel.[1]

Initial studies of the fundamental properties of neptunium phosphates have been preformed to better design actinide separation and purification processes.[2,3] Additionally, there has been interest stemming from use of phosphates for the long term storage of actinides.[4–10] However, few neptunium phosphates have been prepared as pure phases.[11–16] More recently, actinide phosphonates have been explored owing to their possible uses in these nuclear processes.[17–22]

A similar, yet relatively unexplored, area of actinide chemistry is that of actinide phosphites. Although phosphate and phosphite exhibit somewhat similar geometries and bond lengths, the removal of one oxygen atom provides a unique opportunity for new coordination chemistry. To date few actinide phosphites have been synthesized, and most make use of organic templates.[23–28] Actinide phosphite chemistry is also of interest because comparisons can be made with the solid state chemistry of other actinide oxoanion systems that contain C_{3v} anions, including selenite,[29] tellurite,[30] and iodate.[31] Phosphite is also a C_{3v} anion, and here the lone pair found on the aforementioned anions has been replaced by a hydrogen atom. However, the chemistry of phosphite is expected to be markedly different from that of anions such as selenite or iodate, because these anions are mild to strong oxidants, and phosphite is a strong reductant. Therefore, one would expect phosphite to stabilize the tetravalent oxidation state, whereas selenite and iodate generally yield penta- or hexavalent oxidation states. Herein we provide data that supports these suppositions with a series of isotypic thorium(IV), uranium(IV), and neptunium(IV) phosphites, with general formula $An^{IV}(HPO_3)_2(H_2O)_2$ (An^{IV} = Th, U, Np), and a new caesium neptunium(IV) phosphate, $Cs[Np^{IV}(H_{1.5}PO_4)(PO_4)]_2$.

Results and Discussion

Crystals of $Cs[Np(H_{1.5}PO_4)(PO_4)]_2$ obtained appeared light green in color when illuminated by standard room lighting, but under microscope lighting, the single plate-like crystals were light pink. This type of dichroism is common in Np^{IV} compounds, and is termed the Alexandrite effect. The resulting single phase product is shown in Figure 1, and the crystallographic information is shown in Table 1.

[a] Department of Civil Engineering and Geological Sciences and Department of Chemistry and Biochemistry, University of Notre Dame,
156 Fitzpatrick Hall, University of Notre Dame, Notre Dame, Indiana 46556, USA
Fax: +1-574-631-9236
E-mail: talbrec1@nd.edu
[b] Institut für Geowissenschaften, Universität zu Kiel,
Ludevig-Meyn Str. 10, 24118 Kiel, Germany
[c] Forschungszentrum Jülich GmbH, Institute for Energy and Climate Research (IEK-6),
52428 Jülich, Germany

Supporting information for this article is available on the WWW under http://dx.doi.org/10.1002/ejic.201100464.

All of the Np^{VI} from the starting material was reduced by P^{3+} to Np^{IV}, which reacted with the oxidized phosphate to form the product.

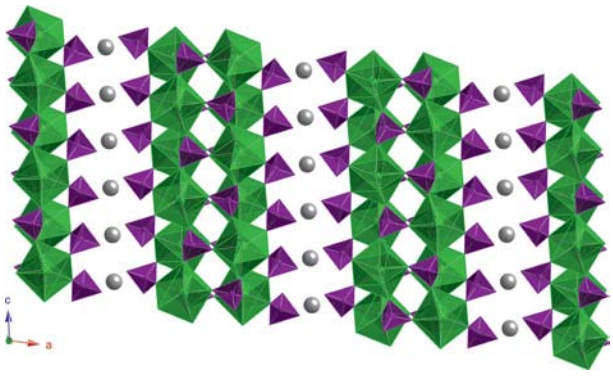

Figure 1. $Cs[Np(H_{1.5}PO_4)(PO_4)]_2$ viewed in the *ac* plane as a double layer of neptunium(IV) phosphate with caesium cations in the interlayers. Here the NpO_8 units form edge-sharing chains. These then form a double-layered sheet by way of the phosphate units. The Np^{IV} atoms are shown as green polyhedra, the phosphate anions are purple polyhedra, and the caesium atoms are shown in light gray.

Table 1. Crystallographic data for $Cs[Np(H_{1.5}PO_4)(PO_4)]_2$ (**A**), $Np(HPO_3)_2(H_2O)_2$ (**B**), $U(HPO_3)_2(H_2O)_2$ (**C**), and $Th(HPO_3)_2(H_2O)_2$ (**D**).

Compound	**A**	**B**	**C**	**D**
Mass	986.79	432.99	429.99	422.99
Color and habit	light pink plate	pale green column	dark green block	colorless block
Space group	*C*2/*c* (No. 15)	*Pbca* (No. 61)	*Pbca* (No. 61)	*Pbca* (No. 61)
a /Å	29.449(4)	8.6672(8)	8.70230(10)	8.8482(2)
b /Å	6.5800(8)	9.0152(5)	9.05920(10)	9.1711(2)
c /Å	10.964(3)	18.267(2)	18.3558(3)	18.5259(5)
α /°	90	90	90	90
β /°	98.700(2)	90	90	90
γ /°	90	90	90	90
V /Å^3	1323.4(3)	1427.3(2)	1447.10(3)	1503.33(6)
Z	4	8	8	8
T /K	100(2)	100(2)	103(2)	100(2)
$\rho_{calcd.}$ /g cm^{-3}	4.953	4.030	3.947	3.747
μ(Mo-K_α) /cm^{-1}	189.03	150.12	228.77	202.65
R(F) for $F_o^2 > 2\sigma(FB_o^2)$[a]	0.0239	0.0154	0.0170	0.0424
$R_w(FB_o^2)$[b]	0.0472	0.0296	0.0441	0.1257
CSD number	423001	423002	423004	423003

[a] $R(F) = \Sigma||F_o| - |F_c||/\Sigma|F_o|$. [b] $R_w(F_o^2) = \{\Sigma[w(F_o^2 - F_c^2)^2]/\Sigma wF_o^4\}^{1/2}$.

This neptunium(IV) structure is based on double layers formed by NpO_8 and PO_4 polyhedra (Figure 1). The NpO_8 groups have approximate C_{2v} symmetry (see Supporting Information for values) with a bicapped trigonal prismatic geometry determined using the algorithm developed by Raymond and coworkers.[32,33] The NpO_8 units are linked by their edges into a 1D chain, which then form double layers through PO_4 tetrahedral groups.

In $Cs[Np(H_{1.5}PO_4)(PO_4)]_2$ there is only one crystallographically unique position for neptunium. It is eight-coordinate with six corner-sharing phosphates and one edge-sharing phosphate, which contributes the last two bridging oxygen atoms. The average Np–O bond length from the corner-sharing phosphates is 2.306(4) Å, whereas the average Np–O bond length of the edge-sharing phosphates is considerably longer at 2.504(4) Å (Table 2). The first coordination sphere of the Np^{IV} atom is shown in Figure 2. Caesium cations balance the charge in the interlayer space. See Supporting Information for more information on the structure and bond valence sum calculations.

Table 2. Selected bond lengths for $Cs[Np(H_{1.5}PO_4)(PO_4)]_2$.

Bond lengths (Å) for $Cs[Np(H_{1.5}PO_4)(PO_4)]_2$			
Np(1)–O(7)	2.216(4)	Cs(1)–O(8)″	3.311(4)
Np(1)–O(6)	2.239(4)	Cs(1)–O(8)‴	3.311(4)
Np(1)–O(4)	2.315(4)	Cs(1)–O(4)	3.678(4)
Np(1)–O(3)	2.338(4)	Cs(1)–O(4)′	3.678(4)
Np(1)–O(1)	2.362(4)	Cs(1)–O(5)	3.806(5)
Np(1)–O(2)	2.365(4)	Cs(1)–O(5)′	3.806(5)
Np(1)–O(2)′	2.471(4)	P(1)–O(6)	1.519(4)
Np(1)–O(3)	2.536(4)	P(1)–O(7)	1.520(4)
Cs(1)–O(5)	3.032(4)	P(1)–O(3)	1.547(4)
Cs(1)–O(5)′	3.032(4)	P(1)–O(2)	1.551(4)
Cs(1)–O(5)″	3.203(5)	P(2)–O(1)	1.515(4)
Cs(1)–O(5)‴	3.203(5)	P(2)–O(4)	1.521(5)
Cs(1)–O(8)	3.297(5)	P(2)–O(5)	1.532(4)
Cs(1)–O(8)′	3.297(5)	P(2)–O(8)	1.588(5)

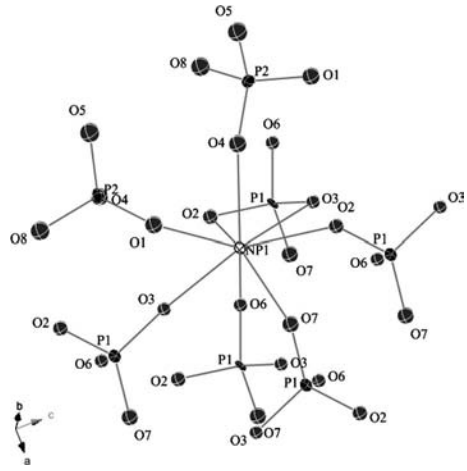

Figure 2. A thermal ellipsoid representation (90% probability) of the neptunium(IV) center in $Cs[Np(H_{1.5}PO_4)(PO_4)]_2$ showing the six corner-sharing and one edge-sharing phosphate anions. The Np^{IV} atom is shown in white, phosphorus atoms are in black, and oxygen atoms are in gray.

Crystals of the first neptunium phosphite $Np(HPO_3)_2(H_2O)_2$ were obtained in similar conditions as the neptunium(IV) phosphate, described above, but Np^{V} was used as a starting material instead of Np^{VI}. In this case, the neptunium is reduced by only one electron, leaving more of the phosphite to react with the now reduced Np^{IV}. As a result, a completely different product was obtained, but it was not pure. The majority of the crystalline product was this new neptunium(IV) phosphite, and approximately 20% of the reaction mixture was found to be $Cs[Np(H_{1.5}PO_4)(PO_4)]_2$, both by solid state UV/Vis/NIR spectroscopy and single-crystal X-ray diffraction.

The pale green crystals of $Np(HPO_3)_2(H_2O)_2$ obtained were suitable for single-crystal X-ray diffraction, and a portion of this structure is shown in Figure 3. The structure is a dense 3D framework based on corner-sharing Np^{IV} and P^{III} polyhedra. The resulting NpO_8 groups have approximate D_{2d} symmetry with trigonal dodecahedral geometry.[32,33] Six corner-sharing phosphite anions and two bound water molecules surround each neptunium atom. The local environment of the Np atoms in the structure of $Np(HPO_3)_2(H_2O)_2$ is shown in Figure 4. The average bond length for the bridging oxygen atoms is 2.301(2) Å, and the average bond length for the bound water molecules is 2.473(3) Å (Table 3). Hydrogen atoms were located from the difference maps for both the bound water molecules and the phosphite centers.

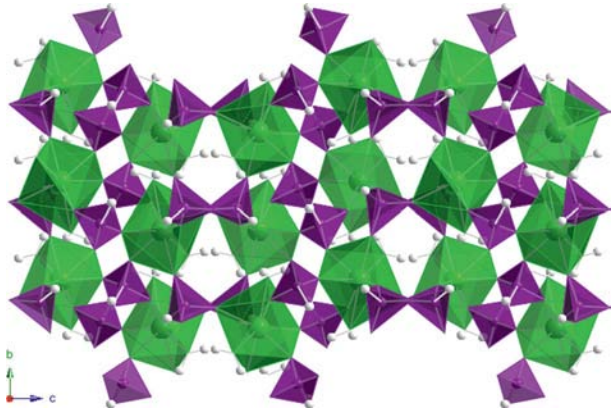

Figure 3. A depiction of the 3D network of $An(HPO_3)_2(H_2O)_2$ (An = Th, U, Np) in the *bc* plane. The $Np^{IV}(HPO_3)_2(H_2O)_2$ structure is shown here but all three are isotypic. Np^{IV} polyhedra are green, the phosphite polyhedra are purple, and the hydrogen atoms are shown in white.

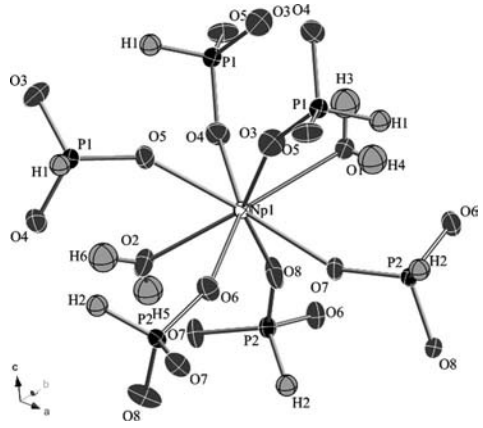

Figure 4. The neptunium center in $Np(HPO_3)_2(H_2O)_2$ is shown in a thermal ellipsoid (90% probability) representation. The neptunium center has two bound water molecules and six corner-sharing phosphite tetrahedra. This structure is the same for the other two actinide phosphites, save for the protons on the bound waters which were not found from the difference maps for U^{IV}/Th^{IV} phosphites. The Np^{IV} atom is shown in white, the phosphorus atoms are in black, the oxygen atoms are in dark gray, and the hydrogen atoms are in light gray.

Table 3. Selected bond lengths for $An(HPO_3)_2(H_2O)_2$.

Bond lengths (Å) for $An(HPO_3)_2(H_2O)_2$	An = Np^{4+}	An = U^{4+}	An = Th^{4+}
An(1)–O(8)	2.249(2)	2.251(3)	2.316(7)
An(1)–O(3)	2.260(2)	2.262(3)	2.332(7)
An(1)–O(6)	2.289(2)	2.296(3)	2.347(7)
An(1)–O(4)	2.315(2)	2.323(3)	2.378(7)
An(1)–O(5)	2.345(2)	2.360(3)	2.393(7)
An(1)–O(7)	2.350(2)	2.380(3)	2.410(7)
An(1)–O(2)	2.454(2)	2.498(3)	2.531(7)
An(1)–O(1)	2.491(3)	2.528(3)	2.574(7)
P(1)–O(5)	1.516(2)	1.509(3)	1.508(7)
P(1)–O(3)	1.516(2)	1.522(3)	1.519(8)
P(1)–O(4)	1.528(2)	1.523(3)	1.524(7)
P(2)–O(7)	1.517(2)	1.513(3)	1.511(8)
P(2)–O(8)	1.520(2)	1.516(3)	1.518(8)
P(2)–O(6)	1.528(2)	1.527(3)	1.538(7)

The $U(HPO_3)_2(H_2O)_2$ and $Th(HPO_3)_2(H_2O)_2$ structures are isotypic with $Np(HPO_3)_2(H_2O)_2$. Both of these phases where obtained using similar conditions. The crystal structures of both show eight-coordinate U^{IV} or Th^{IV} centers. The six corner-sharing phosphite anions and two bound water molecules coordinate the actinide cations [as in $Np(HPO_3)_2(H_2O)_2$ in Figure 4, see also Supporting Information]. Unlike in the structure of Np^{IV} phosphite, protons could not be established on the bound water molecules for the U^{IV}/Th^{IV} phosphite structures. The average U–OH_2 bond length is 2.513(3) Å and 2.312(3) Å for the bridging phosphite oxygens. Longer distances of 2.553(7) Å for Th–OH_2 and 2.363(7) Å for the bridging phosphites are found in the Th structure. The UO_8 and ThO_8 groups within these structures also have approximate D_{2d} symmetry.[32,33]

As shown in Figure 5, transitions consistent with the Np^{IV} oxidation state are observed in the solid state UV/Vis/NIR spectra of $Cs[Np(H_{1.5}PO_4)(PO_4)]_2$ and $Np(HPO_3)_2(H_2O)_2$; especially those at approximately 720 and 950 nm.[22,34,35] Interestingly, the peaks for the neptunium phosphite are shifted to higher wavelengths than the neptunium phosphate peaks. The reason for this shift could be due to the different coordination environment at the two Np^{IV} centers. Although both are eight-coordinate, the

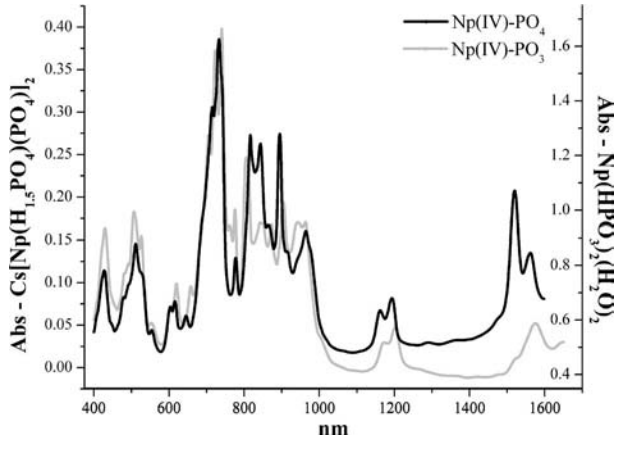

Figure 5. Solid state UV/Vis/NIR spectra for $Np(HPO_3)_2(H_2O)_2$, shown in gray, and $Cs[Np(H_{1.5}PO_4)(PO_4)]_2$, shown in black.

phosphite has two bound water molecules, whereas the phosphate has only bridging oxygen atoms from phosphate anions.

All three of the actinide phosphite compounds described above are isotypic. The thorium phosphite synthesis involved no redox chemistry, whereas the uranium phosphite required an excess of phosphite, and the neptunium phosphite required moving from Np^{VI} to Np^{V} in order to obtain the desired product. Table 4 shows a comparison of the unit cells, volumes, and average bond lengths for the three phosphites, with U^{IV} phosphite compared to Th^{IV} phosphite and Np^{IV} phosphite compared to U^{IV} phosphite. The expansion in bond lengths from neptunium to uranium to thorium is consistent with actinide contraction.

Table 4. Comparison of the unit cells and bond lengths for $An(HPO_3)_2(H_2O)_2$ (An = Th, U, Np).

Actinide	Th	U	Np
a /Å	8.848	–0.146	–0.035
b /Å	9.171	–0.112	–0.044
c /Å	18.526	–0.170	–0.089
V /Å^3	1503.35	–56.25	–19.80
Average An-OH_2	2.553	–0.040	–0.039
Average An-O	2.363	–0.051	–0.011

The phosphite phases described above are quite similar to a thorium(IV) phosphate, $Th(HPO_4)_2(H_2O)$, synthesized by Garcia et al.[36] The unit cells are very close to the dimensions of $Th(HPO_4)_2(H_2O)$ and they share the same *Pbca* space group [*a* = 9.1987(3), *b* = 18.6418(6), *c* = 8.7890(3) Å]. Looking at the overall structure (Figure 6) one can see how similar they are. Here it can be seen how in the absence of cations, phosphite can quite easily mimic phosphate in these densely packed structures.

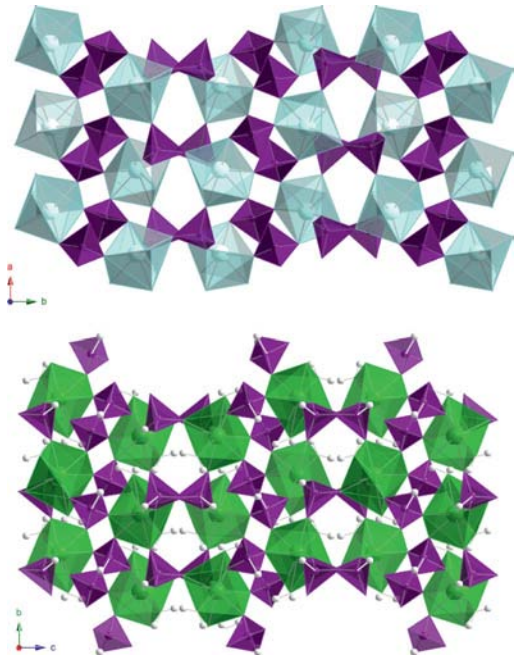

Figure 6. A comparison of the structure of $Th(HPO_4)_2(H_2O)$ (top) with that of $Np(HPO_3)_2(H_2O)_2$ (bottom). The two structures are similar even though the bonding environments of the metal centers are different, with eight-coordinate Np (shown in green) and seven-coordinate Th (shown in aqua).

Although the actinide phosphites and the thorium phosphate structures have different ligands, both PO_4^{3-} and HPO_3^{2-} are essentially tetrahedral and the phosphorus–oxygen bonds in the phosphite groups are slightly shorter than those of phosphate. The hydrogen atom on the P^{3+} atom in phosphite relaxes the tetrahedral symmetry and allows less than ideal bond angles compared to those of the normal phosphate tetrahedron. Even though the structures appear very similar, the Th^{IV} phosphate centers are seven-coordinate and actinide phosphite centers are eight-coordinate. Regardless of this, in this simple, dense structure the two compounds are quite similar because of same type of heavy element packing (Figure 6).

Conclusions

The hydrothermal reactions of Np^{V} and Np^{VI} with phosphorous acid demonstrate that the formation of crystalline products relies strongly on the solubility of the products formed. Both reactions should have yielded Np^{IV} phosphites, but this is not observed. When the reduction of Np^{VI} to Np^{IV} occurs only one equivalent of the ten equivalents of phosphite added is oxidized from $H_3P^{III}O_3$ to $H_3P^{V}O_4$; nevertheless, the only product obtained from this reaction was $Cs[Np(H_{1.5}PO_4)(PO_4)]_2$. When the reaction is changed to the reduction of Np^{V} to Np^{IV} only half an equivalent of H_3PO_3 is allowed to oxidize. Here we see that the majority (va. 80%) of the product is neptunium(IV) phosphite and the remainder is neptunium(IV) phosphate. It seems clear that the solubility of $Cs[Np(H_{1.5}PO_4)(PO_4)]_2$ is probably much less than that of $Np(HPO_3)_2(H_2O)_2$.

This hypothesis is bolstered by the synthesis of $U(HPO_3)_2(H_2O)_2$. Here much of the uranium was still in the mother liquor, and even when allowed to slowly evaporate, a viscous liquid was all that was obtained. These results may be greatly influenced by pH, which is most likely to be the governing factor on the products formed. Here we have successfully synthesized the first neptunium and thorium phosphites. We have also expanded the chemistry of uranium phosphites. Additionally, we have shown that the source of neptunium and the concentration of phosphite can greatly influence the products formed. Thus far, it seems obvious that solubility is the fundamental property that controls the crystallization of these products and that the pH of the starting solutions may greatly affect the products that form.

Experimental Section

Caution! ^{237}Np ($t_{1/2} = 2.14 \times 10^6$ years) represents a serious health risk owing to its α and γ emission, and especially because of its decay to the short-lived isotope ^{233}Pa ($t_{1/2}$ = 27.0 d), which is a potent β and γ emitter. All studies with neptunium were conducted in a laboratory dedicated to studies on transuranium elements. This laboratory is located in a nuclear science facility and is equipped with HEPA filtered hoods and negative pressure gloveboxes that are ported directly into the hoods. The laboratory is licensed by

the Nuclear Regulatory Commission. All free-flowing solids are manipulated in gloveboxes, and products are only examined when coated with either water or Krytox oil and water. There are significant limitations in accurately determining yield with neptunium because this requires drying, isolating, and weighing a solid, which poses certain risks, as well as manipulation difficulties given the small quantities employed in the reactions. Additionally, although the $UO_2(NO_3)_2{\cdot}6H_2O$ used in this study contained depleted uranium, standard precautions for handling radioactive materials, such as uranyl nitrate and thorium nitrate, should be followed.

Syntheses: $UO_2(NO_3)_2{\cdot}6H_2O$ (International Bio-analytical Industries, Inc.), $Th(NO_3)_4{\cdot}4H_2O$ (Sigma–Aldrich), caesium carbonate (Alfa-Aesar, 99.9%), and phosphorous acid (Alfa-Aesar, 97%) were used as received. $^{237}NpO_{2(s)}$ (99.9%, Oak Ridge) was prepared by the oxidation of triple electrorefined neptunium metal. A stock solution of Np^{VI} nitrate (0.372 M, 5 mg in 50 μL of water) was prepared by first digesting $NpO_{2(s)}$ in 8 M HNO_3 for 3 d at 200 °C (in an autoclave). The resulting solution was reduced to a residue, which oxidizes the neptunium to Np^{VI}. This was then dissolved to yield the desired concentration and then bubbled with ozone to ensure that all of the neptunium was Np^{VI}.

$Cs[Np(H_{1.5}PO_4)(PO_4)]_2$: A reaction mixture of Np^{VI} (50 μL, 175 mmol) from the stock solution, Cs_2CO_3 (11.2 mg, 344 mmol), and H_3PO_3 (14.5 mg, 1.769 mol) was diluted to 0.1 mL with distilled water in a 10 mL PTFE autoclave liner. The reaction mixture yields an approximate molar ratio of 2 Cs_2CO_3:Np^{VI}:10 H_3PO_3. The liner was placed in a stainless steel autoclave, which was sealed and placed in a box furnace. This furnace was heated to 175 °C for 3 d and cooled at a rate of 5 °C per hour. Even when the time of this reaction was shortened to just two hours the same pure neptunium(IV) phosphate phase was obtained. The resulting crystals exhibit the Alexandrite effect where they change color depending on the lighting. In bulk under standard room lighting they appear as light green plates, but under illumination with microscope lighting they become light pink in color.

$$NpO_2^{2+} + 2Cs_2CO_3 + 10H_3PO_3 \xrightarrow[\text{with } 5\,^{\circ}C/h \text{ cooling}]{\substack{100\ \mu L\ H_2O \\ 175\,^{\circ}C,\ 3\ days}} Cs[Np^{IV}(H_{1.5}PO_4)(PO_4)]_2$$

$Np(HPO_3)_2(H_2O)_2$: By changing the starting material from Np^{VI} nitrate to Np^{V} hydroxide the final product can be drastically changed. The Np^{VI} stock solution described above was reduced to Np^{V} with excess $NaNO_{2(s)}$ and precipitated as the hydroxide by adding excess ammonium hydroxide. The resulting $Np^{V}O_2OH_{(s)}$ was washed repeatedly with water to remove all excess nitrate/nitrite. The reaction mixture to prepare $Np(HPO_3)_2(H_2O)_2$ consisted of $Np^{V}O_2OH_{(s)}$ (4.9 mg, 171 mmol), Cs_2CO_3 (11.7 mg, 359 mmol), and H_3PO_3 (14.9 mg, 1.817 mol). This was also diluted to 0.1 mL with distilled water and placed in a 10 mL PTFE autoclave liner. The molar ratio was the same as the reaction described above. The stainless steel autoclave was sealed and placed into a box furnace, which was headed to 175 °C for 3 d and cooled at a rate of 5 °C per hour. The major product was $Np(HPO_3)_2(H_2O)_2$, which was obtained as green, column-like crystals. About 20% of the reaction mixture was light pink plates. This was found to be $Cs[Np(H_{1.5}PO_4)(PO_4)]_2$ by single crystal X-ray diffraction and solid state UV/Vis/NIR spectroscopy.

$$NpO_2^{+} + 2Cs_2CO_3 + 10H_3PO_3 \xrightarrow[\text{with } 5\,^{\circ}C/h \text{ cooling}]{\substack{100\ \mu L\ H_2O \\ 175\,^{\circ}C,\ 3\ days}} Np^{IV}(HPO_3)_2(H_2O)_2$$

$U(HPO_3)_2(H_2O)_2$: $U(HPO_3)_2(H_2O)_2$ was synthesized by loading uranyl nitrate (101.5 mg, 101 mmol), Cs_2CO_3 (130.5 mg, 200 mmol), and H_3PO_3 (330.0 mg, 2.013 mol) into a 23 mL PTFE autoclave liner with 2 mL of distilled water. This yields an approximate ratio of reactants of 2 Cs_2CO_3:U^{VI}:20 H_3PO_3. The liner was then sealed in a stainless steel autoclave and placed into a box furnace. The reaction was then heated to 175 °C for 2 days and then cooled at a rate of 7 °C per hour. The mother liquor from this reaction was very dark green and a few very dark green crystals were obtained. The block crystals were washed with water and the mother liquor was saved.

$$UO_2(NO_3)_2{\cdot}6H_2O + 2Cs_2CO_3 + 20H_3PO_3 \xrightarrow[\text{with } 7\,^{\circ}C/h \text{ cooling}]{\substack{2\ mL\ H_2O \\ 175\,^{\circ}C,\ 2\ days}} U^{IV}(HPO_3)_2(H_2O)_2$$

$Th(HPO_3)_2(H_2O)_2$: $Th(HPO_3)_2(H_2O)_2$ was synthesized by reacting thorium nitrate (114.0 mg, 103 mmol), Cs_2CO_3 (130.0 mg, 199 mmol), and H_3PO_3 (328.2 mg, 2.002 mmol) in 2 mL of distilled water. This gives a ratio of reactants of 2 Cs_2CO_3:Th^{IV}:20 H_3PO_3. The 23 mL PTFE liner was sealed in a stainless steel autoclave and placed into a box furnace. The reaction was heated to 175 °C for 2 d and then cooled at a rate of 7 °C per hour. The product was washed with water and most of the white product obtained was an uncharacterized powder; however, a few colorless, block crystals were found as well. These crystals were easily separated and were suitable for single-crystal X-ray diffraction.

$$Th(NO_3)_4{\cdot}4H_2O + 2Cs_2CO_3 + 20H_3PO_3 \xrightarrow[\text{with } 7\,^{\circ}C/h \text{ cooling}]{\substack{2\ mL\ H_2O \\ 175\,^{\circ}C,\ 2\ days}} Th^{IV}(HPO_3)_2(H_2O)_2$$

Crystallographic Studies: Crystals of all compounds were mounted on CryoLoops with Krytox oil and optically aligned on a Bruker APEXII Quazar X-ray diffractometer using a digital camera. Initial intensity measurements were performed using a IμS X-ray source, a 30 W microfocused sealed tube (Mo-K_α, λ = 0.71073 Å) with high-brilliance and high-performance focusing Quazar multilayer optics. Standard APEXII software was used for determination of the unit cells and data collection control. The intensities of reflections of a sphere were collected by a combination of four sets of exposures (frames). Each set had a different ϕ angle for the crystal and each exposure covered a range of 0.5° in ω. A total of 1464 frames with an exposure time of 10 seconds were used for $Cs[Np(H_{1.5}PO_4)(PO_4)]_2$, 1464 frames with an exposure time of 30 seconds were used for $Np(HPO_3)_2(H_2O)_2$, 1076 frames with an exposure time of 10 seconds were used for $U(HPO_3)_2(H_2O)_2$, and 1000 frames with an exposure time of 10 seconds were used for $Th(HPO_3)_2(H_2O)_2$. SAINT software was used for data integration including Lorentz and polarization corrections. Semiempirical absorption corrections were applied using the program SCALE (SADABS).[37]

Further details on the crystal structure investigation may be obtained from the Fachinformationszentrum Karlsruhe, 76344 Eggenstein-Leopoldshafen, Germany (fax: +49-7247-808-666; e-mail: crysdata@fiz-karlsruhe.de), on quoting depository numbers CSD-423001 to -423003. Selected bond lengths are given in Tables 2 and 3.

UV/Vis/NIR Spectroscopy: UV/Vis/NIR data were acquired from single crystals of $Cs[Np(H_{1.5}PO_4)(PO_4)]_2$ and $Np(HPO_3)_2(H_2O)_2$ using a Craic Technologies microspectrophotometer. Crystals were placed on quartz slides under Krytox oil, and the data were collected from 400 to 1600 nm. The exposure time was auto optimized by the Craic software.

Supporting Information (see footnote on the first page of this article): Atomic coordinates and additional structural information (CIFs). Bond valence sum calculations, symmetry calculations, ad-

ditional figures of $Cs[Np(H_{1.5}PO_4)(PO_4)]_2$, $Th(HPO_3)_2(H_2O)_2$, $U(HPO_3)_2(H_2O)_2$, and $Np(HPO_3)_2(H_2O)_2$, and other comparisons with the Th^{IV} phosphate.

Acknowledgments

We are grateful for support provided by the Materials Science of Actinides, an Energy Frontier Research Center funded by the U.S. Department of Energy, Office of Science, Office of Basic Energy Sciences under Award Number DE-SC0001089.

[1] R. J. Silva, H. Nitsche, *Radiochim. Acta* **1995**, *70*, 377.
[2] T. J. LaChapelle, L. B. Magnusson, J. C. Hindman, National Nuclear Energy Series, Manhattan Project Technical Section, Division 4, Plutonium Project 14B, **1949**, 1097.
[3] T. J. Kimura, *J. Radioanal. Nucl. Chem.* **1990**, *139*, 297.
[4] A. Tabuteau, M. Pages, J. Livet, C. J. Musikas, *J. Mater. Sci. Lett.* **1988**, *7*, 1315.
[5] B. D. Begg, E. R. Vance, S. D. Conradson, *J. Alloys Compd.* **1998**, *271*, 221.
[6] N. Dacheux, A. C. Thomas, B. Chassigneux, E. Pichot, V. Brandel, M. Genet, *Mater. Res. Soc. Symp. Proc.* **1999**, *556*, 85.
[7] N. Dacheux, A. C. Thomas, B. Chassigneux, E. Pichot, V. Brandel, M. Genet, *Cer. Trans.* **1999**, *93*, 373.
[8] D. B. Kitaev, Y. F. Volkov, A. I. Orlova, *Radiochemistry* **2004**, *46*, 211.
[9] Y. F. Volkov, S. V. Tomilin, A. I. Orlova, A. A. Lizin, V. I. Spiryakov, A. N. Lukinykh, *Russ. J. Inorg. Chem.* **2005**, *50*, 1660.
[10] D. M. Wellman, S. V. Mattigod, K. E. Parker, S. M. Heald, C. Wang, G. E. Fryxell, *Inorg. Chem.* **2006**, *45*, 2382.
[11] W. H. Zachariasen, *Acta Crystallogr.* **1949**, *2*, 388.
[12] F. Nectoux, A. Tabuteau, *Radiochem. Radioanal. Lett.* **1981**, *49*, 43.
[13] C. E. Bamberger, R. G. Haire, G. M. Begun, H. E. Hellwege, *J. Less-Common Met.* **1984**, *102*, 179.
[14] T. Z. Forbes, P. C. Burns, *Am. Mineral.* **2006**, *91*, 1089.
[15] T. Z. Forbes, P. C. Burns, *Can. Mineral.* **2007**, *45*, 471.
[16] T. H. Bray, T. A. Sullens, T. Y. Shvareva, R. E. Sykora, R. G. Haire, T. E. Albrecht-Schmitt, *J. Solid State Chem.* **2007**, *180*, 70.
[17] T. H. Bray, A. G. D. Nelson, G. B. Jin, R. G. Haire, T. E. Albrecht-Schmitt, *Inorg. Chem.* **2007**, *46*, 10959.
[18] A. G. D. Nelson, T. H. Bray, W. Zhan, R. G. Haire, T. S. Sayler, T. E. Albrecht-Schmitt, *Inorg. Chem.* **2008**, *47*, 4945.
[19] A. G. D. Nelson, T. H. Bray, T. E. Albrecht-Schmitt, *Angew. Chem.* **2008**, *120*, 6348; *Angew. Chem. Int. Ed.* **2008**, *47*, 6252.
[20] A. G. D. Nelson, T. H. Bray, F. A. Stanley, T. E. Albrecht-Schmitt, *Inorg. Chem.* **2009**, *48*, 4530.
[21] J. Diwu, A. G. D. Nelson, T. E. Albrecht-Schmitt, *Comments Inorg. Chem.* **2010**, *31*, 46.
[22] J. A. Diwu, S. A. Wang, Z. Liao, P. C. Burns, T. E. Albrecht-Schmitt, *Inorg. Chem.* **2010**, *49*, 10074.
[23] A. Chretien, J. C. Kraft, *R. Hebd. Seances Acad. Sci.* **1937**, *204*, 1936.
[24] K. A. Avduevskaya, I. A. Rozanov, V. S. Mironova, *Inorg. Mater.* **1977**, *13*, 1515.
[25] K. A. Avduevskaya, N. B. Ragulina, I. A. Rozanov, *Inorg. Mater.* **1981**, *17*, 834.
[26] M. Doran, S. M. Walker, D. O'Hare, *Chem. Commun.* **2001**, 1988.
[27] J. F. Xu, H. H. Li, Y. N. Cao, C. C. Huang, H. H. Zhang, D. S. Lin, Q. Y. Yang, R. Q. Sun, *Chin. J. Struct. Chem.* **2006**, *25*, 1380.
[28] S. Mandal, M. Chandra, S. Natarajan, *Inorg. Chem.* **2007**, *46*, 7935.
[29] a) M. Koskenlinna, J. Valkonen, *Acta Crystallogr., Sect. C* **1996**, *52*, 1857; b) M. A. Cooper, F. C. Hawthorne, *Can. Mineral.* **2001**, *39*, 797; c) P. M. Almond, S. M. Peper, E. Bakker, T. E. Albrecht-Schmitt, *J. Solid State Chem.* **2002**, *168*, 358; d) T. A. Sullens, P. M. Almond, J. A. Byrd, J. V. Beitz, T. H. Bray, T. E. Albrecht-Schmitt, *J. Solid State Chem.* **2006**, *179*, 1192; e) T. H. Bray, S. Skanthakumar, L. Soderholm, R. E. Sykora, R. G. Haire, T. E. Albrecht-Schmitt, *J. Solid State Chem.* **2008**, *181*, 493.
[30] a) F. Brandstätter, *Z. Kristallogr.* **1981**, *155*, 193; b) P. N. Namboodiri, S. N. Tripathi, *J. Mater. Sci.* **2000**, *35*, 337; c) P. M. Almond, T. E. Albrecht-Schmitt, *Inorg. Chem.* **2002**, *41*, 5495; d) J. D. Woodward, T. E. Albrecht-Schmitt, *J. Solid State Chem.* **2005**, *178*, 2922; e) J. Ling, M. Ward, P. C. Burns, *J. Solid State Chem.* **2011**, *184*, 401.
[31] a) A. Y. Tsivadze, N. N. Krot, B. I. Muchnik, *Proc. Moscow Symp. Chem. Transuranium Elem.* **1976**, *89*; b) A. C. Bean, M. Ruf, T. E. Albrecht-Schmitt, *Inorg. Chem.* **2001**, *40*, 3959; c) R. E. Sykora, S. M. McDaniel, D. M. Wells, T. E. Albrecht-Schmitt, *Inorg. Chem.* **2002**, *41*, 5126; d) T. H. Bray, J. Ling, E. S. Choi, J. S. Brooks, J. V. Beitz, R. E. Sykora, R. G. Haire, D. M. Stanbury, T. E. Albrecht-Schmitt, *Inorg. Chem.* **2007**, *46*, 3663.
[32] A. E. V. Gorden, J. Xu, K. N. Raymond, *Chem. Rev.* **2003**, *103*, 4207.
[33] D. L. Kepert, *Prog. Inorg. Chem.* **1978**, *24*, 179.
[34] P. G. Hagan, J. M. Cleveland, *J. Inorg. Nucl. Chem.* **1966**, *28*, 2905.
[35] H. A. Friedman, L. M. Toth, *J. Inorg. Nucl. Chem.* **1980**, *42*, 1347.
[36] M. A. Salvado, P. Pertierra, G. R. Castro, C. Trobajo, J. R. Garcia, *Inorg. Chem.* **2008**, *47*, 1246.
[37] G. M. Sheldrick, *SADABS, Program for absorption correction using SMART CCD based on Blessing's method*; R. H. Blessing, *Acta Crystallogr., Sect. A* **1995**, *51*, 33.

Received: May 2, 2011
Published Online: August 5, 2011

